Supplementary Information

Nonlinear Current-Voltage Characteristics and Enhanced Negative Differential Conductance in Graphene Field Effect Transistors

Lin Wang*, Xiaoshuang Chen*, Yibin Hu, Anqi Yu, and Wei Lu

National Laboratory for Infrared Physics, Shanghai Institute of Technical Physics, Chinese Academy of Sciences, 500 Yutian Road, Shanghai 200083, China

Synergetic Innovation Center of Quantum Information & Quantum Physics, University of Science and Technology of China, Hefei, Anhui 230026, China

1. The Self-heating Effect and Hot Electron Effect on the Saturation Output

As known to us, self-heating and hot electron effects in conventional GaN or GaAs HEMT play important roles in the output power due to strong electron-phonon interaction and transfer of electrons from channel into the buffer layers at high electric-field, and ultimately lead to the NDC in the saturation region[1, 2]. In ours work, the threshold voltage of NDC in graphene FET is too low to cause significant heating and hot electron trapping effects due to the absence of band gap near Dirac point and larger conduction-band discontinuity at the interface between graphene and insulators (the bandgap of SiO2 and SiC is between 7~9eV). Despite of this, we would like to perform further analysis about the self-heating and hot-electron effects in graphene through self-consistent numerical analysis on the heat-diffusion and non-equilibrium electron-lattice energy system. The intrinsic thermal conductivity of graphene has been investigated rigorously in Refs. 3-5, recently. The temperature and channel length dependencies of graphene 2D thermal conductivity approximately follow the relationship:

$$k = \sum_{p}\left(\frac{A}{LG_{\mathrm{p,ball}}} + \frac{1}{k_{\mathrm{p,diff}}}\right)^{-1} \approx \frac{G_{ball}}{A}\left(\frac{1}{L} + \frac{1}{(\pi/2)\lambda}\right)^{-1} \quad (1)$$

Where p is the phonon mode, $G_{p,ball}$ is the ballistic thermal conductivity, $\underline{k}_{p,diff}$ is the diffusive thermal conductivity (~600$Wm^{-1}k^{-1}$), the second equality in Eq. 1 is the simpler "gray" approximation of the first one with $G_{ball}/A \sim 4.2\times10^{9} WK^{-1}m^{-2}$, and λ is the phonon mean free path in the order of 90nm. Eq. 1 is similar to the mobility reduction during the scaling down the gate length of FET, as proposed in previous works[6]. In free suspended graphene at 300K, the thermal conductivity is 2000~4000$Wm^{-1}K^{-1}$, therefore, the thermal time constant usually less than 1ns. In this Supplementary Information, we seek to extend the drift-diffusion model in the Methods to account for the electro-thermal effects:

$$\vec{J}_{n,p} = -n(p)q\mu_{n,p}(\nabla\phi_{n,p} + P_{n,p}\nabla T) \quad (2)$$

Where $P_{n,p}$ in the order of 1mV/K is the absolute thermoelectric powers according to the Mott formula

$$P_{n,p} = -\frac{\pi^2 k_B^2 T}{3q}\frac{1}{\sigma}\frac{d\sigma}{d\phi_{n,p}} \quad . \tag{3}$$

where k_B is the Boltzman constant, σ is the conductivity. To calculate the temperature distribution in the device due to the self-heating, the following equation is solved assume the thermal equilibrium between electron and lattice system ($T_{n,p}=T_L=T$):

$$c\frac{\partial T}{\partial t} - \nabla \cdot k\nabla T = -\nabla \cdot [(P_n T + \phi_n)\cdot J_n + (P_p T + \phi_p)\cdot J_p] \tag{4}$$

The temperature-dependent mobility due to electron-phonon scattering can be approximated well by a simple analytical model for practical applications, rather than the rigorous *ab initio* density-functional perturbation theory[7, 8]. Here, the temperature dependent mobility in graphene is mainly determined by the acoustic-phonon scattering with mobility $\mu \sim \mu_0(T/T_0)^{-1}$ far from the velocity saturation, and is implemented in the transport model. In addition, as refer to the thermal conductivity of substrate, we adopt the experimentally accepted values range from 0.014W/cm/K to 1W/cm/K, such as SiO2 and SiC. The heat dissipation of graphene channel composed of two parallel paths to the underlying substrate and the metal contact as shown in Fig. 1b, with total thermal resistance $R_{th}=(R_{the}^{-1}+R_{thl}^{-1})^{-1}$. It should be noted that, the thermal resistance of substrate depends on the geometrical structure of the device, in case 1, the hot spot of channel transfers its heat in lateral 3D, while in case 2, only vertical heat-sinking takes place. Therefore, the total thermal resistance can be dominated by the contact when the graphene sheet is in case 2. The output characteristics of graphene self-heating are shown in Fig. S1(a) with thermal conductivity changed from 0.014W/cm/K to 1W/cm/K. It can be found that the current output depends weakly on the substrate, due to the small thermal contact resistance and high thermal conductivity of graphene. In addition, the lattice temperature along the graphene sheet is almost uniform, in well consistent with the Raman mapping in Ref. 5. In Fig. S1a, we have also considered stronger dependence of scattering rate on the temperature (red lines). It is shown that the NDC effect is not affected obviously by the self-heating effect at positions (a, b and c), instead of that, the self-heating effect is possibly to be visualized in the sublinear region. While in Fig. S1a, we have assumed the thermal equilibrium between electron and lattice, however, due to the smaller electron heat capacitance in graphene, the electron temperature is usually higher than that of lattice. Therefore, we have also taken into account the hot electron effect on the NDC of output characteristics through extending the thermodynamic model (2) to the energy balance equation:

$$\frac{\partial W_{n,p}}{\partial t} + \nabla \cdot \vec{S}_{n,p} = \vec{J}_{n,p}\cdot\vec{E}, \text{ and } \frac{\partial W_L}{\partial t} + \nabla \cdot \vec{S}_L = 0 \tag{5}$$

where $S_{n,p}$ is the energy flux given by

$$\vec{S}_{n,p} = -\frac{3}{2}\left(\frac{k_B T}{q}\cdot\vec{J}_{n,p} + \kappa_{n,p}\nabla T_{n,p}\right),\ \vec{S}_L = -k\nabla T_L \tag{6}$$

where $\kappa_{n,p}=Ln(p)q\mu_{n,p}T_{n,p}$ with Lorentz number $L=\pi^2 k_B/3q^2$ is electron (hole) thermal conductivity given by the Widemann-Franz law. Based above results, the output characteristics are shown in Fig. S1c, from which it can be found the NDC-effect is still clearly visible in comparison with those of Fig. S1a. While the strength of NDC effect is a bit weaker than those of Fig. S1a, which is mainly caused by the change of junction resistance and shift of Fermi level at the contact. In Fig.

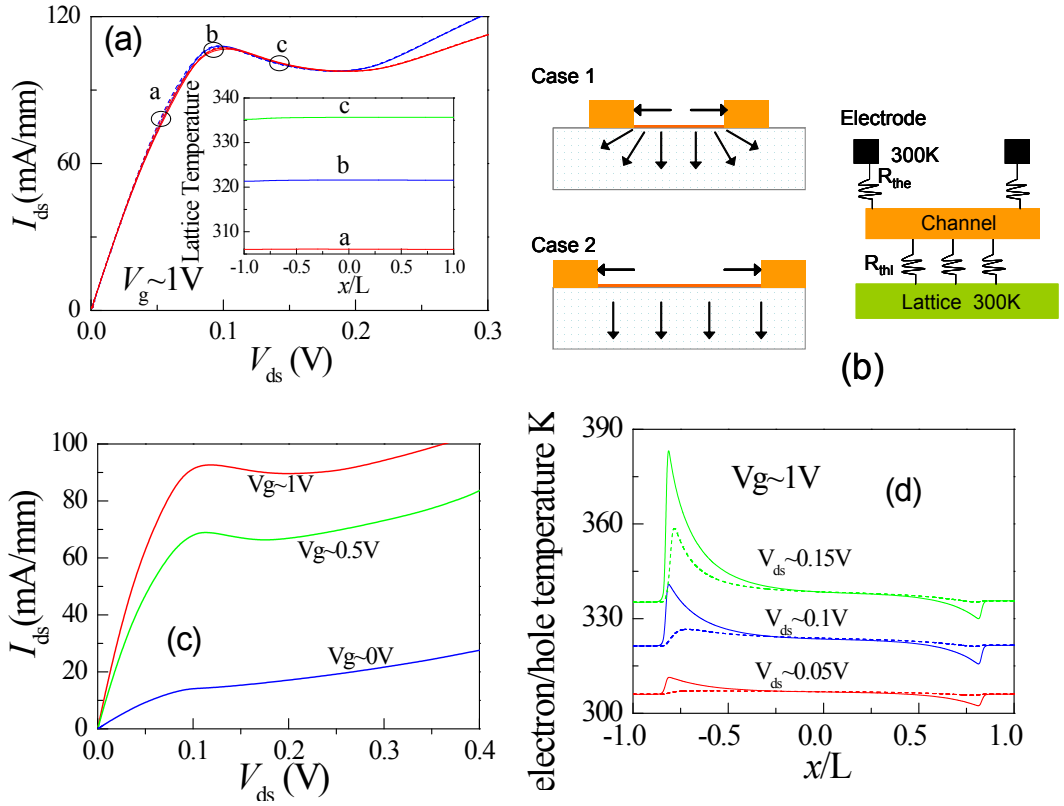

Fig.S1. Self-heating and hot-electron effects on the output characteristics of graphene FET, (a)The self-heating effect ($\mu \propto T^{-\beta}$)on the NDC at different substrate conductivity from 0.014W/m/K to 1W/m/K, the NDC does not change at different conductivities, red lines have larger temperature dependent coefficient (β=2) than blue lines (β=1), (b) is the schematics of heat sinking for different device geometries, case 1 is the result of 3D lateral heat transfer, and case 2 is the vertical heat-sinking, all the processes can be represented by the picture at right side, two parallel paths of heat-sinking are recognized in Fig. S1a. (c)The nonequilibrium thermal process between electron and lattice system, we found that NDC effect is not strongly affected by the hot electron effect in our discussed regime. (d) is the hot electrons (solid lines) and holes (dashed lines) temperature distributions along the channel close to the NDC region.

S1d, we found that the hot electron/hole temperature distributions are non-uniform along the channel, due to the junction resistance and local electric field maximum. Higher temperature will lead to the shift of quasi-Fermi level close to the Dirac point, and thus reduce the junction resistance or NDC effect as inferring from the discussed results in the main text. Despite of this, the heating effect is not strong enough to cause current saturation and emissions of optical phonons, and the NDC proposed in the main text can hold up. To enhance the NDC effect, exploring the polarity of the metal-graphene contact can be an efficient route.

2. Simplified Transport Model in the Linear Regime

From above discussions and the results present in the text, it can be found that the NDC effect as depicted in Fig. S1 is in the low-field regime, where the electron-phonon scattering is not strongly enough to cause the full current saturation. In addition, the self-heating and hot electron trapping-effects in the channel of graphene FET do not lead to the significant change of

the NDC phenomenon proposed in our paper. In conventional semiconductors, the high-field self-heating effect is mainly caused by the strong intrinsic-phonon scattering, while in graphene, the SPP (surface polar-optical phonon) scattering is usually taking place in front of the electron-intrinsic optical-phonon scattering due to its high optical phonon energy (~0.2eV)[9]. Therefore, the only remaining issue affects the NDC effect would possibly be the interface imperfections which has ever been ignored in the main text. To a good approximation in the linear regime, the channel conductivity can be described by

$$\sigma^2=[\mu C_{OX}(V_{TG}-V_{CNP})]^2+\sigma_{min}^2 \quad (7)$$

where σ_{min} is the minimum conductivity determined mainly by the electron-hole puddles, V_{CNP} is the Dirac voltage, which is shift by the applied source-drain voltage V_{ds} following approximately V_{CNP}~V_{CNP0}+kV_{ds} with k between 0.5~1, as can be inferred from the main text that V_{CNP} is corresponding to the formation of p-n junction in the linear regime (seeing Fig. 5b). The drain current can be expressed as

$$I_{ds}=\sigma V_{ds}/L=V_{ds}\sqrt{[\mu C_{OX}(V_{TG}-V_{CNP})]^2+\sigma_{min}^2}/L \quad (8)$$

which gives the output conductance

$$g_{ds}\sim\frac{(\mu C_{OX})^2(V_{TG}-V_{CNP})(V_{TG}-V_{CNP})-kV_{ds}))+\sigma_{min}^2}{\sqrt{[\mu C_{OX}(V_{TG}-V_{CNP})]^2+\sigma_{min}^2}} \quad (9)$$

This analytical expression offers insight into the necessary condition for the NDC, when

$$g_{ds}\sim(\mu C_{OX})^2(V_{TG}-V_{CNP})(V_{TG}-V_{CNP})-kV_{ds}))+\sigma_{min}^2<0 \quad (10)$$

It should be noted that in the above results the p-n junction is not the necessary condition for the NDC effect, as inferred from the main text (Fig. 4a) the conductance minimum can take place in the front of the p-n formation. The condition of NDC can be reduced into the following expressions

$$\frac{3(V_{TG}-V_{CNP0})-\sqrt{(V_{TG}-V_{CNP0})^2-8\frac{\sigma_{min}}{C_{OX}\mu}^2}}{4k}<V_{ds}<\frac{3(V_{TG}-V_{CNP0})+\sqrt{(V_{TG}-V_{CNP0})^2-8\frac{\sigma_{min}}{\mu}}}{4k} \quad (11)$$

Therefore, based on the simplified analytical model, it can be found that the NDC conductance can be enhanced by the reduction of minimum conductance.

REFERENCES

1.N. Braga, R. Mickevicius, R. Gaska, X. Hu, M. S. Shur, M. Asif Khan, G. Simin, and J. Yang, J. Appl. Phys. **2004**, 95, 6409-6413.

2. S. S. IsIam, A. F. M. Anwar. IEEE Trans. Micro. Theo. &Tech. **2004**, 52, 1229-1236.

3. M. Bae, Z. Li, Z. Aksamija, P. N. Martin, F. Xiong, Z. Ong, I. Knezevic, E. Pop. Nature Communications. **2012**, 4, 1734.

4. V. E. Dorgan, A. Behnam, H. J. Conley, K. I. Bolotin, E. Pop. Nano. Lett. **2013**, 13, 4581-4586.

5. M. Freitag, M. Steiner, Y. Martin, V. Perebeinos, Z. Chen, J. C. Tsang, P. Avouris. Nano. Lett. **2009**, 9, 1883-1888.

6. M. S. Shur. IEEE Elec. Dev. Lett. **2002**, 23, 511-513.
7. K. M. Borysenko, J. T. Mullen, E. A. Barry, S. Paul, Y. G. Semenov, J. M. Zavada, M. Buongiorno Nardelli, K. W. Kim. Phys. Rev. B(R). **2010**, 81, 121412.
8. K. M. Borysenko, J. T. Mullen, X. Li, Y. G. Semenov, J. M. Zavada, M. Buongiorno Nardelli, K. W. Kim. Phys. Rev. B(R). **2011**, 83, 161402.
9. V. Perebeinos, P. Avouris, Phys. Rev. B. **2010**, 81, 195442.